DUAL TRANSVERSE AND LONGITUDINAL STREAK CAMERA IMAGING AT ELSA*

M. Switka, F. Frommberger, P. Haenisch, M. Schedler and W. Hillert, ELSA, Bonn, Germany

Abstract

The electron pulse stretcher ring ELSA located at Bonn University provides 0.5–3.5 GeV polarized and non-polarized electron beams for external experimental stations. A streak camera system has been installed to capture time resolved images of beam dynamics ranging from nanoseconds to several milliseconds [1]. Particular attention was drawn to the capability of simultaneous imaging of both transverse beam dimensions, hence providing information of all spatial dimensions in one synchroscan or slow sweep measurement. Incoherent and coherent beam instabilities, especially at high stored beam currents, are subject of analysis due to the planned intensity upgrade towards 200 mA for standard operation. The current resolution performance of the imaging system and machine relevant measurements are presented.

INTRODUCTION

As streak cameras convert three dimensional light beam information into a two dimensional image with aspect on longitudinal resolution, the dimension of one transverse plane is always suppressed, either by the streak action or the narrow slit of the input optics. As for certain events interest arises for capturing dynamics in all three dimensions simultaneously, a method for dual transverse imaging at ELSA was introduced and demonstrated in [2]. In order to test the convenience of such a setup, a low-cost version was installed mostly utilizing equipment already available at the lab. Resolution limits were encountered primarily due to the limiting aperture of the optical system and for very short time windows due to limited light intensity. Furthermore, longitudinal instability behaviour was investigated through grow-damp measurements using the bunch-by-bunch feedback system (BBB). Attention was especially drawn to cavity temperature effects and decoherence observation.

BEAM MANIPULATION AND RECOUPLING

The primary lens of ELSA's *M7* optical synchrotron radiation diagnostic beamline focuses the visible synchrotron radiation onto the focal plane of the first lens of a relay line lens pair. The subsequent beam manipulation section in is illustrated in Fig. 1. The parallel light bundle is split by a 50 % beamsplitter, partially bypassing a Dove prism which rotates the beam transversally by 90°. Both light bundles, upright and flat, are recoupled onto the same light path with slight displacement and angular deviation. The second relay lens focuses the beam onto the streak camera's input slit

($M_{tot} = 0.044$). Hence the two perpendicular electron beam images are projected next to each other. In this setup, two main apertures restrict the resolution of transverse beam dynamics: The 0.15×4.41 mm^2 (v × h) large photo cathode limits the imaging of vertical light beam displacements. Secondly, the rectangular mirror downstream from the Dove prism imposes a horizontal aperture for the flat beam and a vertical aperture for the upright beam. Note that the original beam image orientation is upright.
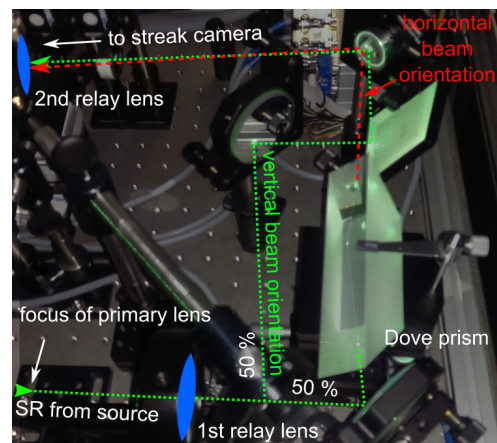
Figure 1: Optical setup for simultaneous imaging of both transverse beam dynamics. One part of the beam is rotated by 90° after exiting the Dove prism.

DUAL TRANSVERSE IMAGING

The streak camera used is the model C10910 by Hamamatsu [3]. Exemplary *slow sweep* measurements for the dual transverse imaging capability are shown in Fig. 2. Parts of
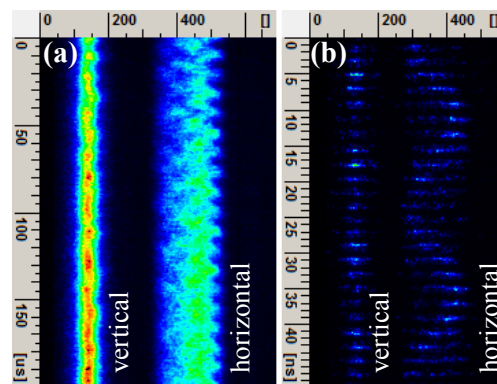
Figure 2: Dual transverse *slow sweep* images. Injection beam dynamics are captured at sufficient SNR (a) and single bunch resolution (b).

the injection process are captured where large horizontal

beam oscillations are expected. Image (a) shows vertical (left streak) and horizontal (right streak) beam dynamics during a time window of 200 μs where the signal-to noise ratio (SNR) is sufficient. Image (b) shows single bunches resolved during a time window of 50 ns. Due to the low irradiation time, the SNR is much lower, yet the horizontal betatron oscillations are observable including partial oscillation decoherence. Note that the intensity fluctuation of the vertical beam is due to the large horizontal oscillation amplitude, causing the signal to partially exceed the aperture perimeter. Further examples can be reviewed in [2].

LONGITUDINAL MEASUREMENTS

Grow-damp measurements were performed in dependency of different beam energies and cavity temperatures. The behaviour at coherent damping was imaged with single bunch resolution.

Obtaining Damping Rates

To utilize the streak camera as quantitative measurement device, data quality of grow-damp measurements was tested against the model for incoherent longitudinal damping:

$$\tau_s = \frac{2ET_{\text{rev}}}{\Delta E_{\text{SR}}\left(2 + \frac{\alpha_c L}{2\pi R}\right)}, \qquad (1)$$

where E is beam energy, T_{rev} revolution period, $\Delta E_{\text{SR}} \propto E^4/R$ energy loss per revolution, α_c momentum compaction, L the ring length and R the bending radius. For this purpose the beam was first stabilized with the BBB in storage mode. It was then excited longitudinally by switching off the BBB for a few milliseconds. The excitation process of the beam was synchronously monitored with the streak camera's *synchroscan* unit. Note that due to image symmetry in *synchroscan* mode only the upper half of the image is presented. Observation indicated that the duration of BBB down time had only negligible effect on the shape or amplitude of the excitation and the damping behaviour. The grow-damp measurements were performed between beam energies of 1 and 3 GeV. A typical measurement is illustrated in Fig. 3.
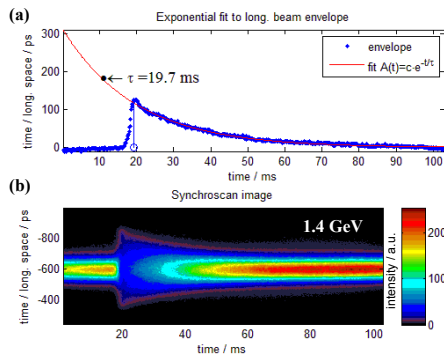
Figure 3: Exemplary grow-damp measurement at 1.4 GeV. An exponential decay function is fit to the upper envelope of the streak camera image.

In order to quantify the damping rate each column of the bitmap image was analyzed from top to bottom. The first value above noise threshold determines the longitudinal position of the beam envelope and links it to the underlying time grid. This assumes that only incoherent oscillations contribute to the amplitude which is only valid as an approximation due to the contribution of coherent oscillations seemingly enlarging the amplitude. However, analysis with the BBB's diagnostics showed a much faster decay of the coherent oscillation in comparison to the incoherent. In order to obtain the exponential fit the envelope of the initially damped beam marks the ground level. The data interval for the fit is set from maximum excitation to the end of the data set. The result is summarized in Fig. 4. The data shows
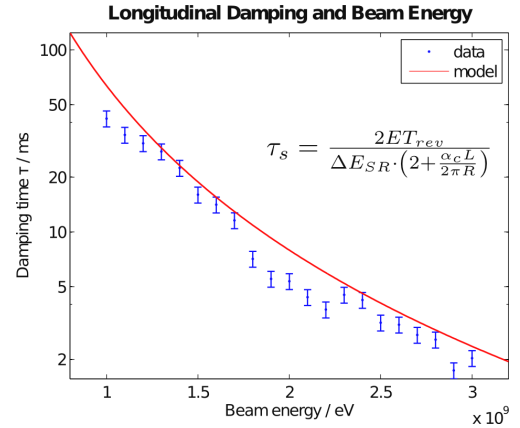
Figure 4: Damping rates at different beam energies.

sufficient agreement with the model. However, it appears that the measured damping time is systematically smaller than the expected value. Up to ten measurements were taken and averaged for one energy. A systematic error estimation of 10% is included, reflecting the effect of different threshold parameters on the damping time as well as the limited vertical pixel resolution.

Temperature Effects

At higher beam energies the shorter damping times prevent the built-up of large oscillation amplitudes which reduces the quality of the taken data. Furthermore, as heat load on the cavity body increases with beam energy, it was observed that the instability behaviour changed significantly with cavity temperature. An exemplary overview is given in Fig. 5, where the BBB down time was 10 ms and no down time repetition was manually set. The beam current was 80 mA.

The repetition rate of the instability occurrence increases to a maximum rate with rising temperature and decreases again as temperature rises further. The coherence duration, amplitude and rise time of the instability change significantly with temperature. At low temperatures a relatively slow collective rising behaviour is observable. At higher temperatures the instability is mostly visible due to instantly appearing incoherent oscillations with lower amplitude.
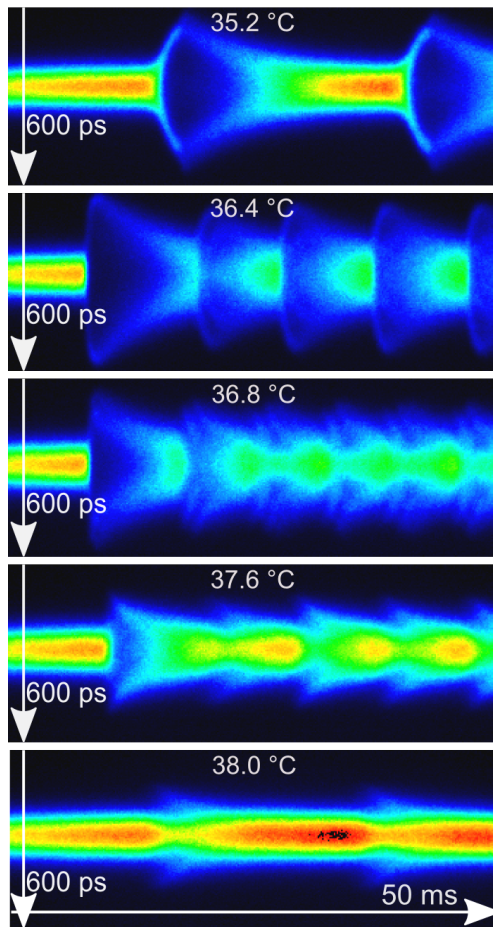
Figure 5: Damping and re-excitation behaviour for different cavity temperatures during grow-damp measurements in 1.9 GeV storage mode.
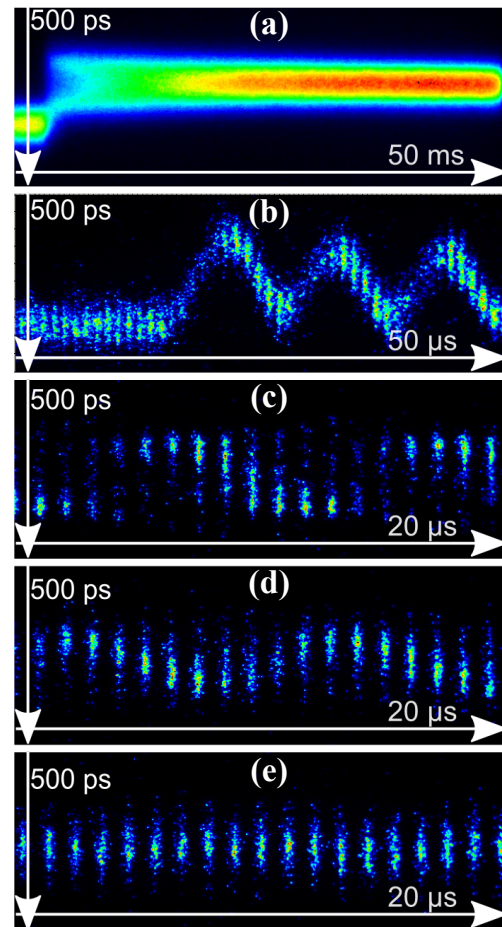
Figure 6: Single bunch oscillation behaviour after cavity phase jump.

Decoherence Observation

As individual bunch dynamics are not observable on millisecond time scales due to streak overlap, the BBB was used to remove all bunches but one. Aside, no instability growth was observed at BBB down time. Therefore the longitudinal oscillation was excited by an RF phase jump as visible in Fig. 6 (a). In (b) the instant of the phase jump is resolved with the maximum time window at which the bunch signals are yet distinguishable. The intensity fluctuation is likely caused by the limiting aperture. In order to gain maximum intensity the beam splitting section was removed and hence horizontal dispersive orbits were not resolved. Images (c) to (e) show the chronological evolution of the oscillation. In (c) the bunch distribution appears somewhat distorted which is likely an artifact due to aperture restriction. The broadening however is clearly visible as decoherence of the oscillation. The BBB is damping the coherent oscillation as visible in (d) and (e).

CONCLUSION

The intensity fluctuation due to the aperture limit has significant influence on the streak camera images. In order to clarify the appearance of artifacts observable as in Fig. 6 (c) both transverse planes need to be measured simultaneously. As beam intensity is not yet sufficient at the ELSA diagnostic beamline, dual transverse synchroscan measurements will be investigated after an aperture increase of the optical transfer line is completed.

REFERENCES

[1] M.T. Switka, et al., Streak Camera Imaging at ELSA, contribution IBIC 2013, Oxford

[2] M.T. Switka, et al., Synchrotron Radiation Diagnostics Performance at ELSA, contribution IPAC 2014, Dresden

[3] Hamamatsu Streak Camera C10910 data sheet: http://www.hamamatsu.com/resources/pdf/sys/ SHSS0016E07_C10910s.pdf